Monthly Notices
of the
ROYAL ASTRONOMICAL SOCIETY

Mon. Not. R. Astron. Soc. **414,** 1285–1291 (2011) doi:10.1111/j.1365-2966.2011.18463.x

Hydrogen and oxygen adsorption on a nanosilicate – a quantum chemical study

T. P. M. Goumans[1]★ and Stefan T. Bromley[2,3]

[1]*Gorlaeus Laboratories, Leiden Institute of Chemistry, Leiden University, PO Box 9502, 2300 RA Leiden, the Netherlands*
[2]*Departament de Química Física and IQTCUB, Universitat de Barcelona, Martí i Franquès 1, E-08028 Barcelona, Spain*
[3]*Institució Catalana de Recerca i Estudis Avançats (ICREA), E-08010 Barcelona, Spain*

Accepted 2011 February 2. Received 2011 January 12; in original form 2010 September 27

ABSTRACT

The reactivity of the thermodynamically stable nanopyroxene cluster $Mg_4Si_4O_{12}$ towards hydrogen and oxygen atoms is studied. Quantum chemical calculations reveal that it can adsorb hydrogen atoms without a barrier, which could catalyze H_2 formation. Furthermore, if we consider consecutive atom adsorption, $Mg_4Si_4O_{12}$ can take up to the equivalent of four units of water (2H + O) before molecular water starts to form preferentially. The resulting superoxygenated nanosilicate cluster ($Mg_4Si_4H_4O_{16}$) contains only hydroxyl groups and has a high oxygen-to-metal ratio of 2 compared to bulk silicates (1.33–1.5). The hydroxylated cluster readily adsorbs even more oxygen atoms in the form of chemisorbed molecular water; however, the molecular water will readily photodesorb in the diffuse interstellar medium. The large oxygen-uptake capacity of nanosilicates could contribute to the large oxygen depletion observed in diffuse clouds, although depletion into other sources must take place as well. The infrared spectra of the (oxygenated) nanopyroxene are calculated, and we identified its strong infrared transitions. Some of the O–Si–O bending modes have blueshifted from 20 μm in bulk silicates to 14–18 μm in nanosilicates. The hydroxylated nanopyroxenes all have sharp, strong features in the 9–12 μm region and the $Mg_4Si_4H_4O_{16}$ cluster has a moderately strong feature around ∼25 μm due to frustrated OH rotations. These distinct infrared features may eventually lead to the identification of (hydroxylated) nanosilicates in stellar outflows, interstellar clouds and/or protoplanetary discs.

Key words: astrochemistry – molecular processes – ISM: abundances – ISM: atoms – ISM: molecules.

1 INTRODUCTION

Silicate dust grains, in particular olivines ($Mg_xFe_{2-x}SiO_4$) and pyroxenes ($Mg_xFe_{1-x}SiO_3$), are ubiquitous in the interstellar medium (ISM; Draine 2003; Jones 2007). The transformations that these silicate grains undergo in the different stages of the stellar evolutionary cycles are still not fully understood. As stars reach the end of their lives they shed their mass in stellar outflows, leading to silicate formation in oxygen-rich stars. From infrared (IR) emission observations with the *Infrared Space Observatory* (*ISO*) towards evolved stars with medium to high mass-loss rates, it is inferred that; (1) most of these newly formed silicates are Mg-rich (Molster, Waters & Tielens 2002a), (2) a significant fraction (∼10 per cent) is crystalline (Molster et al. 2002a) and (3) enstatite ($MgSiO_3$) is more abundant than forsterite (Mg_2SiO_4) (Molster et al. 2002b).

While the ISM is thus refuelled with crystalline enstatite and forsterite grains from these stellar outflows, these must subsequently be efficiently amorphized since in the ISM only amorphous silicates are observed of mainly olivinic composition (Kemper, Vriend & Tielens 2004; Molster & Kemper 2005). Strong [supernovae (SNe)] shock waves could amorphize and shatter dust grains by ion implantation and sputtering (Demyk et al. 2001; Carrez et al. 2002a; Kemper et al. 2004; Molster & Kemper 2005) although cosmic rays can also induce *crystallization* (Carrez et al. 2002b; Szenes et al. 2010).

Conversely, as diffuse clouds contract to form dark clouds in which eventually new generations of stars are born, a significant fraction of the silicates in the protoplanetary discs of young stellar objects (YSOs) appear to be crystalline again (van Boekel et al. 2004). In contrast to the crystalline silicates around evolved stars, forsterite is more abundant than enstatite in the colder outer regions of the disc (Bouwman et al. 2008). Recent *ISO* observations of active and quiescent phases of EX Lupi have established that silicate

★E-mail: t.goumans@chem.leidenuniv.nl

crystallization may be induced by thermal heating in solar outbursts (Abraham et al. 2009).

To summarize, when new silicate dust grains are formed in the stellar outflows of dying stars, they are partly crystalline and these crystalline grains are Mg-rich with a higher concentration of pyroxene (enstatite) than olivine (forsterite). As these dust grains are processed by shocks and sputtering in the ISM, they are amorphized and become mostly olivinic. When the dust grains are eventually incorporated into protoplanetary discs around the YSO, they are partly crystallized again, possibly by stellar outbursts, with a higher concentration of crystalline forsterite than enstatite at larger radii.

In the condensation, destruction and coagulation stages of silicates, nanoclusters could play an important role. Indeed, a substantial ($\sim$10 per cent) mass fraction of the silicate grain population in the diffuse ISM could be very small ($<$15 Å diameter) (Li & Draine 2001). Recently, Cherchneff & Dwek (2010) have modelled the chemistry of the very first stages of dust nucleation, i.e. molecular cluster formation, in Population III SN ejecta, in particular small binary metal oxide clusters. While the structure and stability of nano-sized clusters of silicon dioxide and magnesium oxide have been extensively studied using accurate computational modelling (Bromley et al. 2009), the structure and stability of mixed nanosilicates such as pyroxenes and olivines are much less well established theoretically (Woodley 2009). The formation of these mixed interstellar silicates likely occurs through coagulation of the binary oxides (Kamitsuji et al. 2005).

Nano-sized silicates and other oxides have very dissimilar optical, electronic, chemical and thermodynamic properties from their bulk counterparts (Johnston 2002; Bromley et al. 2009; Catlow et al. 2010). Indeed, the mixing energies of MgO and SiO_2 are very different at the nanoscale and in the bulk. In this paper, we study the structure and stability of the nanopyroxene with the most favourable mixing energy, the nanopyroxene $Mg_4Si_4O_{12}$. This thermodynamically favourable nanopyroxene may be a significant constituent of the diffuse ISM, potentially formed in stellar outflows as well as from sputtering and fragmentation of larger dust grains. We study its reactivity towards the abundant hydrogen and oxygen atoms, which could contribute to H_2 formation and oxygen depletion, respectively. We also report the most intense IR bands of the bare, hydrogenated and oxygenated clusters which may eventually lead to the positive detection of nanosilicates in the diffuse ISM.

2 STABILITY OF NANOSILICATES

We studied the structure and stability of the first eight members of the $(MgO)_n(SiO_2)_n$ and $(MgO)_{2n}(SiO_2)_n$ series, which are nanoclusters of the Mg-rich pyroxene and olivine family (enstatite and forsterite, respectively). To establish the ground-state geometry of these nano-sized clusters, we employ the well-established Monte Carlo-basin hopping (MC-BH) global optimization technique (Wales & Doye 1997) with atomistic pair potentials specifically parametrized for nanoscale silicates and MgO (Roberts & Johnston 2001; Flikkema & Bromley 2003; Hassanali & Singer 2007). Due to the high availability of oxygen in the clusters, the metal centres and hydrogen are all assumed to be oxidized and all resulting non-bonding cation–cation interactions are treated purely electrostatically (with effective charges: Si +2.4, Mg +1.2, H +0.6 and O −1.2). The MC-BH runs all used a fixed maximum step size of $\sim$1 Å and temperatures ranging between 1000 and 10 000 K. The highest temperature MC-BH runs of up to 50 000 steps were first used with random initial cluster geometries of the relevant composition in order to broadly sample the energy landscape. A selection of approximately 10 optimized geometries was then taken from these runs, and for each structure longer MC-BH runs (up to 500 000 steps) were performed at intermediate temperatures. Finally, lower energy candidate structures from these secondary runs were used as initial seeds for the lowest temperature searches in an attempt to exhaustively explore particularly stable regions of the potential energy landscape. Of the several hundreds of candidate structures thus generated, 20–40 of the most promising structures were further optimized with density functional theory (DFT; Frisch 2004) at the B3LYP/6-31G* (Stephens et al. 1994) level.

In order to assess the relative energetics of forming nanoscale $(MgO)_n(SiO_2)_n$ and $(MgO)_{2n}(SiO_2)_n$ clusters with respect to the corresponding bulk magnesium–silicate crystalline structures, we calculating their mixing enthalpies as follows: (i) for the clusters the total energy of the mixed cluster was compared with the proportional sum of the energies of the $(MgO)_n$ and $(SiO_2)_n$ ground-state clusters (e.g. $E_{\rm mix} = E[(MgO)_n(SiO_2)_n] - [E(MgO)_{2n}/2 + E(SiO_2)_{2n}/2]$) and (ii) for the solid phases the total energy of the bulk magnesium silicate was compared with the proportional sum of the energies of α-quartz silica and rocksalt MgO. For the bulk crystal structures, the calculated[1] mixing enthalpy is much more favourable for forsterite (−0.59 eV) than for orthoenstatite (−0.29 eV) in good agreement with experiment (−0.65 and −0.32 eV, respectively; Zaitsev et al. 2006). Therefore, under thermodynamical mixing conditions of MgO and SiO_2, forsterite would be the predominant mineral. With a solar Mg/Si ratio of 1.07 (Anders & Grevesse 1989) the preferential formation of forsterite (Mg/Si = 2) would leave room for the formation of silica, which indeed has been observed around T-Tauri stars (Sargent et al. 2009).

Surprisingly, however, the nanosilicate mixing energies showed a minimum for the nanopyroxenes (i.e. nanoscale mixing is more favourable than bulk mixing) but not for the nano-olivines. This minimum corresponds to the nanopyroxene $Mg_4Si_4O_{12}$ cluster (Fig. 1) which has the lowest mixing energy of all the nanoclusters we studied (−0.49 eV). Because this nanocluster is thermodynamically favoured under nanoscale mixing conditions, it could well be a constituent of the diffuse ISM, either directly from stellar outflows or from processing of larger grains. We further investigate the reactivity of this nanopyroxene towards hydrogen and oxygen atoms and study its IR properties.

3 REACTIVITY OF NANOPYROXENE $Mg_4Si_4O_{12}$ WITH H AND O

Nanosilicate grains could adsorb or absorb hydrogen and oxygen atoms in the diffuse ISM if the sorption energies are sufficiently high to prevent thermal and/or photodesorption. Previous calculations have established that H and O can chemisorb ($E_{\rm ads} >$ 1 eV) barrierlessly on a bare forsterite surface, and H_2O is also bound strongly ($E_{\rm ads} \sim$ 1 eV) (Muralidharan et al. 2008; Goumans, Catlow & Brown 2009a; Goumans et al. 2009b). Because, in general, nanoparticles have undercoordinated surface atoms, we anticipate the binding energies for H and O atoms on the nanosilicates to be even higher.

[1] Based on calculations with the CRYSTAL code (Saunders et al., CRYSTAL 2006, University of Torino) with B3LYP with a large basis and converged *k*-point sampling.

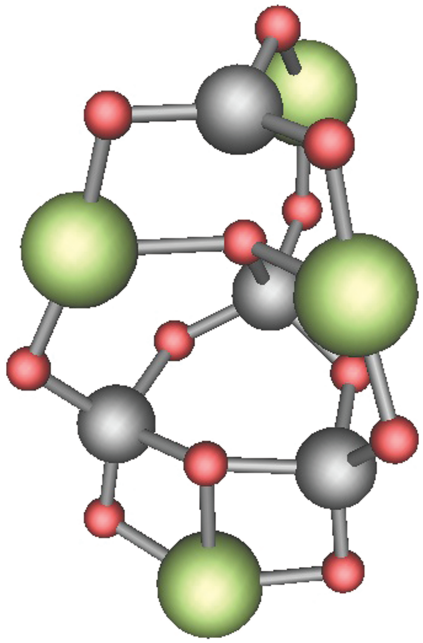

Figure 1. The most stable nanopyroxene cluster $Mg_4Si_4O_{12}$. Si: grey, Mg: green, O: red.

3.1 Adsorption of first H and O atoms

We first studied the adsorption of O and H atoms separately, and then the sequential addition of O, H and H atoms. The first H atom can bind, without a barrier, at various positions on the $Mg_4Si_4O_{12}$ cluster with adsorption energies between 0.8 and 2.0 eV. These chemisorbed H atoms can be easily removed again by incoming gaseous H atoms to yield H_2 via the Eley–Rideal mechanism, just as was calculated for the bare forsterite surface (Goumans et al. 2009a). Therefore, this nanopyroxene, and very likely all nanosilicates, can catalyze the formation of H_2 in the diffuse ISM by barrierlessly adsorbing one H atom, which reacts barrierlessly with a second H atom to yield H_2. Since in this two-step process the large formation energy of H_2 (4.5 eV) is broken up, this process could be more efficient than via the recombination of two physisorbed H atoms on graphitic grains (Langmuir–Hinshelwood formation).

Ground-state triplet oxygen atoms, O(^{3}P), can also adsorb barrierlessly on the $Mg_4Si_4O_{12}$cluster with a large adsorption energy of 2.14 eV, and this adsorbate can be further stabilized (−0.65 eV) by relaxation to the singlet state. O(^{3}P) initially bridges in between two Mg atoms, but upon relaxation to the singlet ground state of the $Mg_4Si_4O_{13}$ cluster, a peroxo (O_2^{2-}) type linkage is formed.

The oxygenated nanopyroxene can react with a gaseous H atom in a very exothermic (−4.38 eV), barrierless reaction. During this adsorption process the peroxo bond is broken up, yielding back the original oxide (O^{2-}) and a strongly bound bridging OH unit [E_{ads} (OH) = 2.74 eV]. Reaction of this hydroxylated cluster $Mg_4Si_4O_{12}$(OH) with another H atom is again barrierless and very exothermic (−4.91 eV), yielding a second OH group, preferentially over the formation of either H_2 or H_2O. Therefore, the bare nanopyroxene $Mg_4Si_4O_{12}$ catalyzes H_2 formation via chemisorbed H atoms, but once it becomes oxygenated through sorption of an oxygen atom, the two subsequent incoming H atoms preferentially form OH units rather than H_2, yielding a hydroxylated nanosilicate.

It is instructive to compare the total adsorption energy of the O and two H atoms on the nanopyroxene (12.08 eV) to the formation energy of molecular water from these atoms (9.46 eV). The uptake of 2H + O atoms to yield the $Mg_4Si_4O_{12}H_2O$ cluster is thus favoured by 2.61 eV over H_2O formation – an adsorption energy that far exceeds that of molecular water (∼1 eV) on bulk silicates (Muralidharan et al. 2008; Goumans et al. 2009a,b). Using the MC-BH search technique, we found two $Mg_4Si_4O_{12}H_2O$ cluster structures that are even more stable (H_2O adsorption energies of 3.26 and 3.14 eV). Whilst these clusters are not very dissimilar from those obtained by sequential additions (O, H, H) to the most stable $Mg_4Si_4O_{12}$ cluster at the most favourable positions, we have not established the mechanism nor the activation energies for the transformation between these structures. However, it is not unreasonable that for the first and subsequent adsorption of oxygen atoms on the $Mg_4Si_4O_{12}$ cluster the preferential thermodynamic equilibrium structure will be reached eventually by the excess reaction energies of adsorption, hydrogenation, dehydrogenation and further energetic processing in the diffuse ISM.

3.2 Adsorption of further O and H atoms

From our detailed atomistic study of the adsorption of the first H and O atoms, we conclude that in an H-rich environment such as the ISM the thermodynamically stable product for every O adsorption will be accompanied by two H adsorptions, yielding two stable OH units (or eventually molecular H_2O), while any excess hydrogenation will be eventually negated by preferential H_2 formation. Rather than trying to find the detailed pathways for every intermediate cluster, we searched for the minimum-energy structure of the hydroxylated $Mg_4Si_4O_{12}(H_2O)_n$ (n = 1–5) clusters using the MC-BH technique.

Since H_2O is energetically the most stable product of H and O atoms in the gas phase (H_f = –9.46 eV), we report in Table 1 the average adsorption energy per unit molecular H_2O, $\langle E_{ads}(H_2O)\rangle$, as a measure of the stability of the oxygenated, or rather hydroxylated, nanosilicate cluster. The total energy, E_{tot}, of the $2n$ H + n O atoms reacting with the $Mg_4Si_4O_{12}$ cluster to yield $Mg_4Si_4O_{12}(H_2O)_n$ amounts to $-\ n \times [\langle E_{ads}(H_2O)\rangle + 9.46\,\text{eV}]$, also reported in Table 1.

As illustrated by the $\langle E_{ads}(H_2O)\rangle$ values in Table 1, the adsorption of the first oxygen atom, accompanied by two hydrogen atoms, is by far the most energetically favoured. Up to four oxygen atoms

Table 1. Calculated adsorption energies (eV) of ($2n$ H + n O) atoms on $Mg_4Si_4O_{12}$ reported as average adsorption energy of H_2O, $\langle E_{ads}(H_2O\rangle$, and total reaction energy E_{tot} (see the text). Both energies are given for the two lowest energy clusters of the respective composition according to the DFT calculations. The energetic ranking of the clusters in each set of two (optimized using interatomic potentials) is also given in the final column with respect to the lowest energy cluster found in the MC-BH runs.

n	$\langle E_{ads}(H_2O)\rangle$	E_{tot}	MC-BH ranking
1	3.26	−12.72	5
	3.14	−12.60	9
2	2.62	−24.18	2
	2.52	−23.97	3
3	2.62	−36.25	17
	2.50	−35.90	9
4	2.42	−47.53	3
	2.41	−47.51	14
5	1.91	−56.87	2
	1.71	−55.87	1

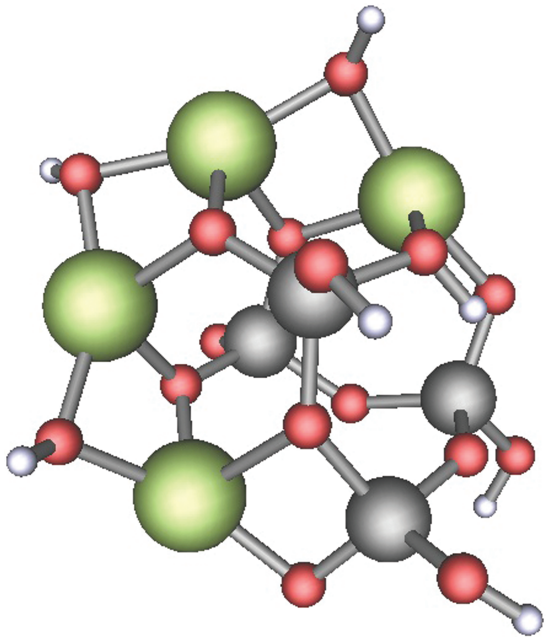

Figure 2. The energetically favourable hydroxylated nanopyroxene cluster $Mg_4Si_4O_{12}(H_2O)_4$. Si: grey, Mg: green, O: red, H: white.

are adsorbed on the nanosilicate with an average $\langle E_{ads}(H_2O)\rangle$ of over 2 eV, still much higher than the adsorption of molecular water on a bulk silicate surface (∼1 eV) or on water ice (∼0.5 eV). It is remarkable that none of these lowest energy structures up to $Mg_4Si_4O_{12}(H_2O)_4$ have molecular H_2O adsorbed on the surface, but only contain surface hydroxyls (OH) instead (Fig. 2). These hydroxylated clusters are thus likely to be more resistant to water photodesorption as opposed to pure water ice (Öberg et al. 2009). If a fifth oxygen atom is incorporated, however, invariably molecular water is formed in the lowest energy structure, which could relatively easily be removed via photodesorption ($E_{des} = 1.6$ eV), but is too strongly bound for thermal desorption.

On the basis of these relative energies, it is plausible that in the diffuse ISM the reaction of $Mg_4Si_4O_{12}$ with multiple O and H atoms would ultimately lead to the formation of the superoxygenated $Mg_4Si_4O_{12}(H_2O)_4$ cluster (Fig. 2), which is a hydroxylated nanosilicate. Further hydrogenation and oxygenation of this cluster will only lead to the formation of the molecular species H_2 and H_2O. Once the interstellar cloud becomes opaque enough to prevent water photodesorption, however, the hydroxylated nanosilicate could start to retain molecular water ice. At higher densities, these nanograins are also more likely to coagulate in larger structures, eventually forming more bulk-like silicates.

4 IR FEATURES OF THE (HYDROXYLATED) NANOPYROXENE

In Fig. 3, we have plotted parts of the scaled (Scott & Radom 1996) calculated IR spectra of the lowest energy $Mg_4Si_4O_{12}$ and $Mg_4Si_4O_{12}(H_2O)_4$ clusters that are related to the Si–O stretch and O–Si–O bending features. It should be noted that the plots of the calculated IR spectra have been Lorentzian-broadened for illustration purposes only. Towards astronomical objects, the actual line shapes will strongly depend on the local physical conditions (temperature, velocity, luminosity, etc.). In Table 2, we report the strongest calculated IR features of the $Mg_4Si_4O_{12}(H_2O)_n$ clusters for $n =$ 0–4, with intensities of $>5 \times 10^{-17}$ cm/molecule. In Appendix S1, see Supporting Information, the calculated IR spectra of the $Mg_4Si_4O_{12}(H_2O)_n$ clusters for $n = 1$–3 are shown as well as the full list of IR peaks.

Frequency analysis of the nanopyroxene incorporating up to four extra oxygen atoms and eight hydrogen atoms indicates that there is no absorption in the 3-μm ice band. Rather, almost all OH groups are non-hydrogen bonded and consequently their frequencies around ∼2.7 μm (3800 cm^{-1}) are quite weak ($<1.7\ 10^{-17}$ cm/molecule). Only for the $Mg_4Si_4O_{12}(H_2O)_4$ complex do hydrogen bonds start to appear, but the only adsorption peak at 2.8 μm is still an order of magnitude weaker (3.3×10^{-17} cm/molecule) than the 3-μm water ice feature (20×10^{-17} cm/molecule; Gerakines et al. 1995). As noted by Whittet (2010), the hydroxyl vibrations in the 2.6–2.8 μm range are in fact quite difficult to probe spectroscopically. For the $Mg_4Si_4O_{12}(H_2O)_4$ cluster we find that there is a moderately strong bond, corresponding to frustrated OH rotations (Fig. 4), centred around 24.8 μm (inset of Fig. 3), which could be indicative of hydroxylated (nano)silicates.

All nanopyroxenes have features in the 14–18 μm region which correspond to O–Si–O bend modes. Some of the O–Si–O bending modes are blueshifted with respect to bulk silicate modes because the silica tetrahedra are much more constrained in the nanostructures. The Si–O stretch features around 10 μm contain only a few intense bands, and all hydroxylated nanopyroxenes show strong features centred around 11 μm alongside those at 10 μm. While an ensemble of nanosilicates, consisting of different sizes, stoichiometry and hydroxylation, will smoothen many of the distinct absorption or emission features of the individual clusters, especially at high temperatures and velocities in stellar outflows, perhaps the features around 11 μm and between 14 and 18 μm, which are absent for bulk silicates, could lead to the positive identification of nanosilicates in the ISM. Likewise, the 25-μm feature corresponding to frustrated OH rotations on the hydroxylated nanopyroxene (Fig. 4) could lead to the identification of hydroxylated silicates in the diffuse ISM.

5 DISCUSSION

Nanosilicates are fundamental intermediates in the formation of silicate dust grains in stellar outflows, and they may be ubiquitous in the ISM. Indeed, up to 10 per cent of the mass of interstellar silicates may be in <15-Å sized particles (Li & Draine 2001). These nanoparticles could have persisted from their formation in interstellar outflows, but they could also partly have formed from interstellar processing of larger grains. Since nanoscale properties often differ succinctly from bulk properties, we have studied quantum chemically the structure and reactivity of nanosilicates.

Specifically, we have investigated the structure and reactivity of a very small cluster of enstatite composition, $Mg_4Si_4O_{12}$, which has the most favourable mixing energy for MgO and SiO_2 particles in the nanoregime. This nanosilicate, like a bulk forsterite surface (Goumans et al. 2009a), adsorbs H atoms strongly without a barrier, catalyzing H_2 formation by breaking up the H_2 formation energy in steps and by coupling of the hot intermediates to vibrational modes of a third body.

The nanocluster also strongly adsorbs O atoms, after which the next two H atoms are preferentially incorporated into the cluster rather than yielding H_2. In this sequence of adsorptions, the nanosilicate effectively has adsorbed H_2O, although no molecular water is formed until more than four oxygen atoms have been incorporated. The molecular water that is eventually formed on the

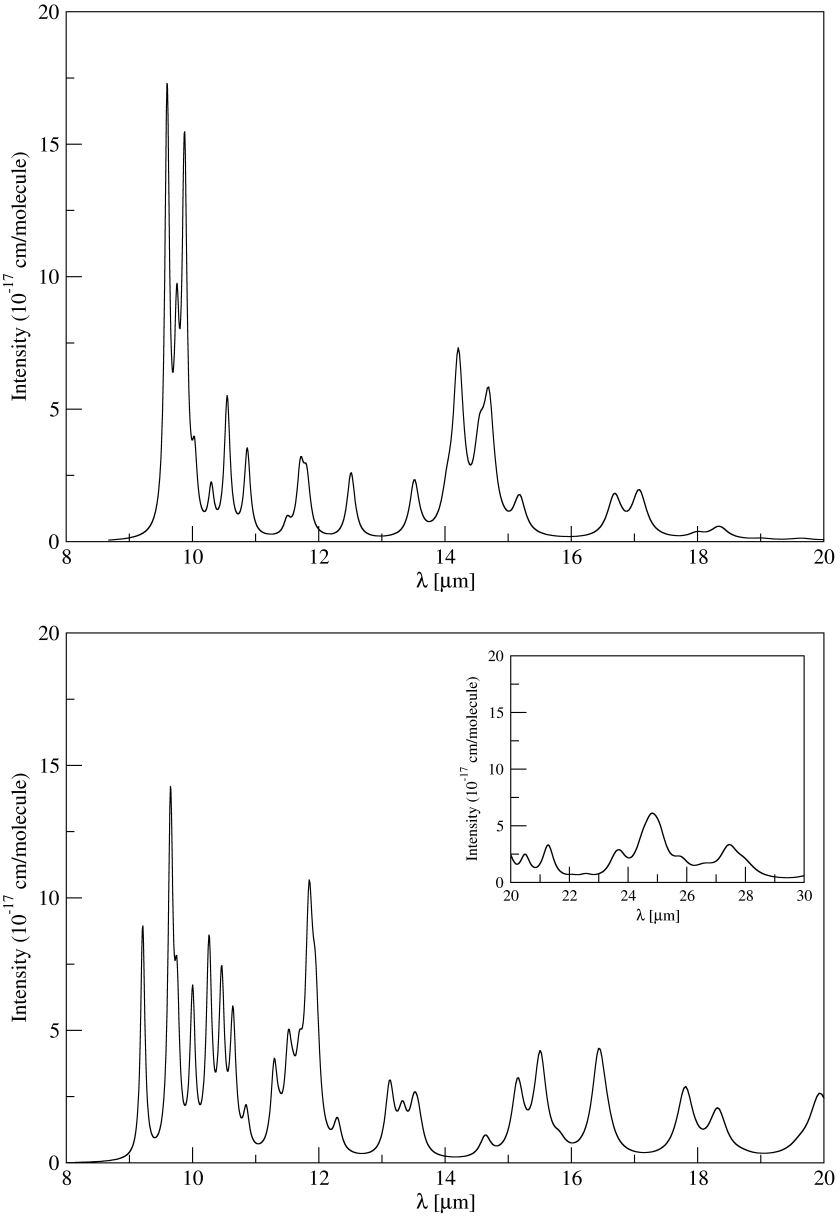

Figure 3. Calculated IR spectra [Lorentzian band profiles from GAUSSVIEW, λ scaled by 1/0.9614 (Scott & Radom 1996)] of $Mg_4Si_4O_{12}$ (top) and $Mg_4Si_4O_{12}(H_2O)_4$ clusters (bottom) in the 8–20 μm region and 20–30 μm region for $Mg_4Si_4O_{12}(H_2O)_4$ (bottom, inset). Spectra of $Mg_4Si_4O_{12}(H_2O)_n$, $n = 1,2,3$, are reported in the Supporting Information.

$Mg_4Si_4O_{12}(H_2O)_5$ cluster is strongly bound (1.6 eV), but is likely to photodesorb readily at low visual extinction in the diffuse ISM.

The high oxygen uptake capacity of the nanosilicate under study, with an oxygen-to-metal ratio (O/M) of 2 for $Mg_4Si_4O_{12}(H_2O)_4$, is interesting in view of the recent observations that oxygen depletes more strongly than other elements towards high total depletion regions (Jenkins 2009; Whittet 2010). In the denser regions, more oxygen ($\sim 2.4 \times 10^{-4} \times n_H$) seems to be tied up in solids than can be incorporated in silicates (Mg + Si abundance $\sim 8 \times 10^{-5}\, n_H$) with a bulk O/M ratio of 1.33 (olivines) to 1.5 (pyroxenes). If indeed 10 per cent of the interstellar silicate mass consisted of nano-sized particles and these could incorporate extra O atoms up to an O/M ratio of 2, substantially more O could be tied up in these superoxygenated nanosilicates. However, this extra oxygen sink would still not suffice to account for the extreme depletion of O.

Porous, fluffy aggregates of (nano)silicates could incorporate more elemental and molecular oxygen in their interior and, at higher visual extinction, molecular water could start forming on the surfaces of these (nano)silicates and their aggregates. Because of the strong binding energy of H_2O ($\geq$1 eV) on these ionic surfaces, it is anticipated that at low coverages there would not yet be a strong ice band. Therefore, as an interstellar cloud starts to become denser, molecular water would be adsorbed on silicate surfaces before the onset of water ice formation in the dense molecular clouds where eventually a catastrophic freeze-out from the gas phase is observed (Whittet et al. 2001; Hollenbach et al. 2009).

Nanosilicates (Carrez et al. 2002a), by virtue of their higher surface-to-volume ratio, can adsorb relatively more molecular water than bulk silicates. Combined with their apparent capacity to adsorb more oxygen atoms, they could be an unidentified depleted oxygen

Table 2. Calculated strong ($I > 5 \times 10^{-17}$ cm/molecule) IR bands (μm), scaled by 1/0.9614 (Scott & Radom 1996) and their intensities (10^{-17} cm/molecule) for $Mg_4Si_4O_{12}(H_2O)_n$ clusters, $n = 0$–4. All calculated IR absorptions are reported in the Supporting Information.

n	Band	Intensity
0	9.60	16.47
	9.75	6.60
	9.88	14.04
	10.55	5.17
	14.21	6.58
1	9.66	10.45
	9.83	12.19
	9.92	9.66
	10.34	9.29
	11.26	5.87
	11.71	8.14
2	9.47	15.71
	10.29	10.15
	10.89	5.19
	11.86	6.52
3	9.67	18.54
	9.88	5.60
	10.04	11.43
	10.26	5.70
	11.44	6.74
	11.67	6.15
4	9.21	8.77
	9.65	13.14
	9.75	5.17
	10.00	5.87
	10.26	7.64
	10.46	6.34
	11.85	8.44

carrier (Whittet 2010), although it is likely that there are other unidentified solid particulates or molecules that contribute to the strong depletion of oxygen as well.

The reported IR features of the (hydroxylated) nanopyroxene show sharp features in the 9–12 and 14–18 μm regimes. While the distinct IR features in 9–11 μm may be overwhelmed by amorphous and/or crystalline bulk silicates, the absorption and emission of these nanosilicates around 12 μm and in the 14–18 μm window may eventually lead to their detection in stellar outflows, in the diffuse ISM or in protoplanetary discs.

ACKNOWLEDGMENTS

This work is financially supported by the Netherlands Organisation for Scientific Research (NWO) through a VENI-fellowship (700.58.404) for TPMG, Spanish Ministry of Science and Innovation grant FIS2008-02238 and Generalitat de Catalunya grants 2009SGR1041 and XRQTC for STB, and by COST Action CM0805 'The Chemical Cosmos: Understanding Chemistry in Astronomical Environments'. Time on Marenostrum via the Barcelona Supercomputer Center is also acknowledged. We would like to thank Ewine van Dishoeck and Xander Tielens for useful discussions.

REFERENCES

Abraham P. et al., 2009, Nat, 459, 224
Anders E., Grevesse N., 1989, Geochimica Cosmochimica Acta, 53, 197
Bouwman J. et al., 2008, ApJ, 683, 479
Bromley S. T., Moreira I. D. R., Neyman K. M., Illas F., 2009, Chemical Soc. Rev., 38, 2657
Carrez P., Demyk K., Cordier P., Gengembre L., Grimblot J., D'Hendecourt L., Jones A. P., Leroux H., 2002a, Meteoritics Planet. Sci., 37, 1599
Carrez P., Demyk K., Leroux H., Cordier P., Jones A. P., D'Hendecourt L., 2002b, Meteoritics Planet. Sci., 37, 1615
Catlow C. R. A., Bromley S. T., Hamad S., Mora-Fonz M., Sokol A. A., Woodley S. M., 2010, Phys. Chemistry Chemical Phys., 12, 786
Cherchneff I., Dwek E., 2010, ApJ, 713, 1
Demyk K. et al., 2001, A&A, 368, L38

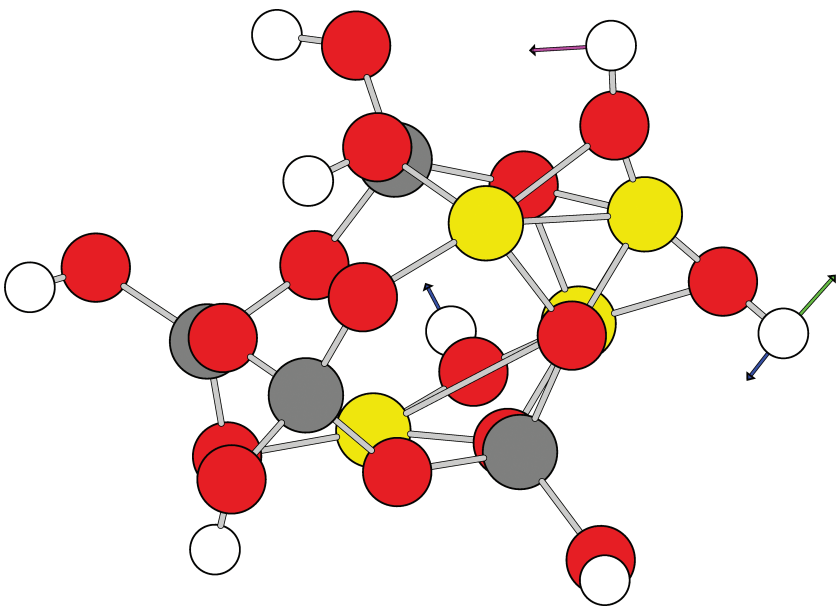

Figure 4. The three most intense IR modes centred around 25 μm for the $Mg_4Si_4O_{12}(H_2O)_4$ cluster (see the inset of Fig. 3), corresponding to frustrated OH rotations. Vibration normal modes: 25.1 μm: blue, 24.8 μm: green, 24.5 μm: purple. Atoms: Si: grey, Mg: yellow, O: red, H: white.

Draine B. T., 2003, ARA&A, 41, 241
Flikkema E., Bromley S. T., 2003, Chemical Phys. Lett., 378, 622
Frisch M. J. et al., 2004, Gaussian 03, Revision D.01, Gaussian Inc., Wallingford, CT
Gerakines P. A., Schutte W. A., Greenberg J. M., van Dishoeck E. F., 1995, A&A, 296, 810
Goumans T. P. M., Catlow C. R. A., Brown W. A., 2009a, MNRAS, 393, 1403
Goumans T. P. M., Catlow C. R. A., Brown W. A., Kastner J., Sherwood P., 2009b, Phys. Chemistry Chemical Phys., 11, 5431
Hassanali A. A., Singer S. J., 2007, J. Phys. Chemistry B, 111, 11181
Hollenbach D., Kaufman M. J., Bergin E. A., Melnick G. J., 2009, ApJ, 690, 1497
Jenkins E. B., 2009, ApJ, 700, 1299
Johnston R. L., 2002, Atomic and Molecular Clusters. Taylor & Francis, London
Jones A. P., 2007, Eurpoean J. Mineralogy, 19, 771
Kamitsuji K., Suzuki H., Kimura Y., Sato T., Saito Y., Kaito C., 2005, A&A, 429, 205
Kemper F., Vriend W. J., Tielens A., 2004, ApJ, 609, 826
Li A., Draine B. T., 2001, ApJ, 550, L213
Molster F., Kemper C., 2005, Space Sci. Rev., 119, 3
Molster F. J., Waters L. B. F. M., Tielens A. G. G. M., 2002a, A&A, 382, 222
Molster F. J., Waters L. B. F. M., Tielens A. G. G. M., Koike C., Chihara H., 2002b, A&A, 382, 241
Muralidharan K., Deymier P., Stimpfl M., de Leeuw N. H., Drake M. J., 2008, Icarus, 198, 400
Öberg K. I., Linnartz H., Visser R., van Dishoeck E. F., 2009, ApJ, 693, 1209
Roberts C., Johnston R. L., 2001, Phys. Chemistry Chemical Phys., 3, 5024
Sargent B. A. et al., 2009, ApJ, 690, 1193
Scott A. P., Radom L., 1996, J. Phys. Chemistry, 100, 16502
Stephens P. J., Devlin F. J., Chabalowski C. F., Frisch M. J., 1994, J. Phys. Chemistry, 98, 11623
Szenes G., Kovacs V. K., Pecz B., Skuratov V., 2010, ApJ, 708, 288
van Boekel R. et al., 2004, Nat, 432, 479
Wales D. J., Doye J. P. K., 1997, J. Phys. Chemistry A, 101, 5111
Whittet D. C. B., 2010, ApJ, 710, 1009
Whittet D. C. B., Gerakines P. A., Hough J. H., Shenoy S. S., 2001, ApJ, 547, 872
Woodley S. M., 2009, Materials Manufacturing Processes, 24, 255
Zaitsev A. I., Arutyunyan N. A., Shaposhnikov N. G., Zaitseva N. E., Burtsev V. T., 2006, Russian J. Phys. Chemistry, 80, 335

SUPPORTING INFORMATION

Additional Supporting Information may be found in the online version of this article:

Figure A1. IR-spectra $Mg_4Si_4O_{12}(H_2O)_n$ clusters, $n = 1 - 2$
Figure A2. IR-spectrum for $Mg_4Si_4O_{12}(H_2O)_3$ cluster
Table A1. IR bands and their intensities for $Mg_4Si_4O_{12}$
Table A2. IR bands and their intensities for $Mg_4Si_4O_{12}(H_2O)$
Table A3. IR bands and their intensities for $Mg_4Si_4O_{12}(H_2O)_2$
Table A4. IR bands and their intensities for $Mg_4Si_4O_{12}(H_2O)_3$
Table A5. IR bands and their intensities for $Mg_4Si_4O_{12}(H_2O)_4$

Please note: Wiley-Blackwell are not responsible for the content or functionality of any supporting materials supplied by the authors. Any queries (other than missing material) should be directed to the corresponding author for the article.

This paper has been typeset from a Microsoft Word file prepared by the author.